

DRAFT: DO NOT CITE OR QUOTE



Draft for open comment

Tropospheric Ozone Assessment Report: Present-day distribution and trends of tropospheric ozone relevant to climate and global atmospheric chemistry model evaluation

Author Team: A. Gaudel, O. R. Cooper, G. Ancellet, B. Barret, A. Boynard, J. P. Burrows, C. Clerbaux, P.-F. Coheur, J. Cuesta, E. Cuevas, S. Doniki, G. Dufour, F. Ebojje, G. Foret, O. Garcia, M. J. Granados-Muñoz, J. Hannigan, F. Hase, B. Hassler, G. Huang, D. Hurtmans, D. Jaffe, N. Jones, P. Kalabokas, B. Kerridge, S. Kulawik, B. Latter, T. Leblanc, E. Le Flochmoën, W. Lin, J. Liu, X. Liu, E. Mahieu, A. McClure-Begley, J. L. Neu, M. Osman, M. Palm, H. Petetin, I. Petropavlovskikh, R. Querel, N. Rahpoe, A. Rozanov, M. G. Schultz, J. Schwab, R. Siddans, D. Smale, M. Steinbacher, H. Tanimoto, D. Tarasick, V. Thouret, A. M. Thompson, T. Trickl, E. Weatherhead, C. Wespes, H. Worden, C. Vigouroux, X. Xu, G. Zeng, J. Ziemke

The Tropospheric Ozone Assessment Report (TOAR) is a current IGAC activity (<http://www.igacproject.org/activities/TOAR>) with a mission to provide the research community with an up-to-date scientific assessment of tropospheric ozone's global distribution and trends from the surface to the tropopause.

Guided by this mission, TOAR has two goals:

- 1) Produce the first tropospheric ozone assessment report based on the peer-reviewed literature and new analyses.
- 2) Generate easily accessible, documented data on ozone exposure and dose metrics at hundreds of measurement sites around the world (urban and non-urban), freely accessible for research on the global-scale impact of ozone on climate, human health and crop/ecosystem productivity.

The report is being written as a series of eight stand-alone publications to be submitted for peer-review to *Elementa: Science of the Anthropocene*, an open-access, non-profit science journal founded by five US research Universities and published by University of California Press (www.elementalscience.org). Prior to submission each paper will be posted to the TOAR webpage (<http://www.igacproject.org/activities/TOAR/OpenComments>) for a 30-day open comment period. We invite members of the atmospheric and biological sciences communities as well as the general public to read the papers and provide comments if they wish to do so. The open comment period will last for 30 days for each paper, with the draft papers posted to the website as they become available.

To provide comments on this particular paper, please send an e-mail to lead author Audrey Gaudel: Audrey.Gaudel@colorado.edu

Table 2.4. Details of the TCO products discussed in this paper.

| Product name and institution | Horizontal resolution of gridded products | Horizontal coverage | Vertical range (tropopause definition) | Temporal resolution/time of day | Record length |
|--|--|--------------------------------|--|---|---|
| OMI/MLS <i>NASA GSFC</i> | 1°x 1.25° | 60°S - 60°N | Surface to tropopause (WMO 2 K km ⁻¹ lapse-rate) | Monthly/ Seasonal 13:45 | 2004 – 2016, continuing |
| GOME & OMI <i>Smithsonian Astrophysical Observatory (SAO)</i> | 1°x 1.25° | 60°S - 60°N | Surface to tropopause (WMO 2 K km ⁻¹ lapse-rate) | Monthly/Seasonal OMI: 13:45 GOME: 10:30 | GOME: 1995 – 6/2003 OMI: 10/2004-2015, continuing |
| OMI-RAL <i>Rutherford Appleton Laboratory (RAL)¹</i> | 5°x 5° | 60°S - 60°N | Surface-450hPa mole fraction and surface to tropopause column (WMO 2 K km ⁻¹ lapse rate) | Monthly/ Seasonal 13:45 | 1995- 2016, continuing |
| IASI-LISA <i>LISA</i> | Averaged over 0.25°x 0.25° grids | Regional (Asia) | Surface-6 and 6-12 km | Seasonal 9:30 | 2008-2014, continuing |
| IASI+GOME2 <i>LISA</i> | 1°x 1° | Regional (Europe, Asia) | Surface to 3 km, and 3-9 km | Monthly/ seasonal 9:30 | 2009-2010 |
| IASI - FORLI <i>Université Libre de Bruxelles and LATMOS/IPSL</i> | Averaged over 5°x 5° grids | 90°S-90°N | Surface to tropopause (WMO 2 K km ⁻¹ lapse rate) | Seasonal 9:30 | 2008 – 2016, continuing |
| IASI - SOFRID <i>CNRS</i> | 5°x 5° | 80°S-80°N | Surface to tropopause (WMO 2 K km ⁻¹ lapse rate) | Seasonal 9:30 | 2008 – 2016, continuing |
| SCIAMACHY | Averaged over grids 1°x 1°, 2°x 2°, 5°x 5° | 80°S-80°N | Tropopause to 60 km (blended tropopause) | Monthly 10:00 | 2002/08-2012/4 |
| FTIR <i>NDACC</i> | Point location | Various sites around the world | Surface to 8 km a.s.l. in this analysis. Retrievals to 45 km are also possible | Monthly/ annual | Earliest data from 1995, continuing |
| Umkehr Umk04+stray light correction, NOAA processing | Point location | Various sites around the world | Surface to 250 hPa | Monthly/annual Morning and afternoon profiles, averaged profile during measurements between 70-90° SZA, latitude and season dependent time of measurements | Earliest data from 1956 at Arosa, Switzerland, continuing |
| TOST | 5°x 5° | 90°S-90°N | Surface to tropopause (WMO 2 K km ⁻¹ lapse rate) | Seasonal/annual | 2008-2012 |

¹ GOME-1, -2A and -2B data in preparation

Table 4.1 Nighttime ozone trends at eight mountaintop sites for winter (DJF), spring (MAM), summer (JJA) and autumn (SON). Bold face indicates trend values that are statistically significant at p-value <0.05. Trend values in parentheses indicate the high and low trend values that bound the 95% confidence interval.

| Site name <i>lat. long. alt.(m a.s.l.)</i> | Years with data | | Trend, full record | p-value | Trend, 2000-2015 | p-value |
|---|-----------------|-----|-----------------------------|-------------|-----------------------------|-------------|
| Mauna Loa <i>19.5°N, 155.6°W</i> <i>3397 m</i> | 1973-2015 | DJF | 0.10 (0.03, 0.21) | 0.01 | -0.05 (-0.63, 0.33) | 0.69 |
| | | MAM | 0.10 (-0.04, 0.23) | 0.15 | 0.60 (0.09, 1.13) | 0.04 |
| | | JJA | 0.16 (0.09, 0.23) | 0.00 | 0.18 (-0.06, 0.40) | 0.14 |
| | | SON | 0.24 (0.14, 0.34) | 0.00 | -0.26 (-0.67, 0.29) | 0.32 |
| Izaña <i>28.3°N, 16.5°W</i> <i>2367 m</i> | 1987 - 2015 | DJF | 0.19 (0.09, 0.28) | 0.01 | 0.00 (-0.16, 0.29) | 1.00 |
| | | MAM | 0.14 (0.02, 0.27) | 0.03 | 0.07 (-0.20, 0.29) | 0.62 |
| | | JJA | 0.14 (-0.02, 0.28) | 0.07 | 0.12 (-0.24, 0.42) | 0.69 |
| | | SON | 0.13 (0.02, 0.21) | 0.02 | 0.06 (-0.16, 0.26) | 0.89 |
| Mt. Waliguan <i>36.3°N, 100.9°E</i> <i>3810 m</i> | 1994 - 2015 | DJF | 0.11 (0.01, 0.20) | 0.04 | 0.08 (-0.10, 0.23) | 0.69 |
| | | MAM | 0.20 (0.10, 0.32) | 0.00 | 0.18 (-0.03, 0.37) | 0.06 |
| | | JJA | 0.19 (-0.06, 0.37) | 0.09 | 0.15 (-0.14, 0.48) | 0.32 |
| | | SON | 0.32 (0.17, 0.36) | 0.00 | 0.32 (0.15, 0.36) | 0.00 |
| Mt Bachelor <i>44.0°N, 121.7°W</i> <i>2763 m</i> | 2004 - 2015 | DJF | too few data | - | too few data | - |
| | | MAM | 0.64 (0.02, 1.24) | 0.05 | 0.64 (0.02, 1.24) | 0.05 |
| | | JJA | 0.77 (-0.11, 1.58) | 0.09 | 0.77 (-0.11, 1.58) | 0.09 |
| | | SON | 1.14 (0.41, 1.70) | 0.01 | 1.14 (0.41, 1.70) | 0.01 |
| Whiteface Mt Summit <i>44.4°N, 73.9°W</i> <i>1483 m</i> | 1975 - 2015 | DJF | too few data | - | too few data | - |
| | | MAM | -0.07 (-0.24, 0.08) | 0.29 | too few data | - |
| | | JJA | -0.38 (-0.49, -0.22) | 0.00 | -0.71 (-1.61, -0.07) | 0.02 |
| | | SON | -0.04 (-0.11, 0.05) | 0.38 | -0.29 (-0.85, 0.12) | 0.13 |
| Jungfrauoch <i>46.5°N, 8.0°E</i> <i>3580 m</i> | 1986 - 2015 | DJF | 0.15 (0.04, 0.29) | 0.01 | -0.07 (-0.21, 0.05) | 0.26 |
| | | MAM | 0.05 (-0.06, 0.19) | 0.30 | -0.15 (-0.24, -0.01) | 0.03 |
| | | JJA | -0.05 (-0.16, 0.11) | 0.42 | -0.12 (-0.37, 0.17) | 0.39 |
| | | SON | 0.13 (0.03, 0.23) | 0.01 | 0.03 (-0.09, 0.14) | 0.56 |
| Zugspitze <i>47.4°N, 11.0°E</i> <i>2962 m</i> | 1978 - 2015 | DJF | 0.31 (0.19, 0.42) | 0.00 | -0.08 (-0.25, 0.05) | 0.12 |
| | | MAM | 0.20 (0.04, 0.35) | 0.01 | -0.27 (-0.34 -0.13) | 0.01 |
| | | JJA | 0.12 (-0.02, 0.28) | 0.08 | -0.20 (-0.49, 0.13) | 0.30 |
| | | SON | 0.15 (0.07, 0.26) | 0.00 | -0.07 (-0.31, 0.10) | 0.44 |
| Summit <i>72.6°N, 38.5°W</i> <i>3212 m</i> | 2000 - 2015 | DJF | 0.02 (-0.26, 0.45) | 0.85 | 0.02 (-0.26, 0.45) | 0.86 |
| | | MAM | -0.32 (-1.04, -0.05) | 0.02 | -0.32 (-1.04, -0.05) | 0.02 |
| | | JJA | too few data | - | too few data | - |
| | | SON | -0.08 (-0.30, 0.14) | 0.32 | -0.08 (-0.30, 0.14) | 0.32 |

Table 5.7 Multi-year mean tropospheric ozone burden (Tg) as measured by ozonesondes and satellites. Also shown is the mean and standard deviation of TOB from the ACCMIP model ensemble for the year 2000 (Young et al., 2013). IASI-FORLI and IASI-SOFRID TOB values for their full latitude range are underestimates due to missing data during polar night.

| | 60° S – 60° N | | | Full latitude range | | |
|---|---------------|---------------|---------------|---------------------|---------------|---------------|
| | 2000 | 2010-2014 | 2014-2016 | 2000 | 2010-2014 | 2014-2016 |
| TOST | | 306 | NA | | 337 | NA |
| | | | | | 90° S – 90° N | |
| OMI/MLS | | 281 | 285 | | - | - |
| OMI-SAO | | 305 | 303 | | | |
| OMI-RAL | | 281 | 287 | | | |
| IASI-FORLI | | 301 | 293 | | 333 | 324 |
| | | | | | 90° S – 90° N | 90° S – 90° N |
| IASI-SOFRID | | 318 | 311 | | 345 | 338 |
| | | | | | 75° S – 75° N | 75° S – 75° N |
| Mean (range), all six products | | 299 (281-318) | | | | |
| Mean (range), five satellite products | | 297 (281-318) | 296 (285-311) | | | |
| ACCMIP model ensemble | 299 ± 21* | | | 337 ± 23 | | |
| | | | | 90°S – 90°N | | |

* Personal communication from Paul Young, Lancaster University

Table 5.8 Availability of all data sets presented in TOAR-Climate.

| <u>In situ observations</u> | |
|---|--|
| Surface ozone observations | The surface ozone values and trends shown in Figures 3.1.1, 3.1.2, 4.1.3 and 4.1.4 (as well as the figures themselves) can be downloaded from: Schultz, MG; Schröder, S; Lyapina, O et al. (2017): Tropospheric Ozone Assessment Report, links to datasets https://doi.pangaea.de/10.1594/PANGAEA.876108 |
| TOST ozonesonde product | The global monthly gridded product is available from the World Ozone and Ultraviolet Radiation Data Centre (WOUDC): http://woudc.org/archive/products/ozone/vertical-ozone-profile/ozonesonde/1.0/tost/ |
| IAGOS commercial aircraft | High resolution IAGOS observations can be downloaded from the IAGOS Data Portal: http://iagos.sedoo.fr/ |
| Mauna Loa Observatory ozone and meteorology | Hourly ozone and meteorological data shown in Figure 4.1.1 are available from NOAA's Global Monitoring Division: https://www.esrl.noaa.gov/gmd/dv/ftpdata.html |
| Lauder, NZ ozonesondes | The ozonesonde data at Lauder are part of WOUDC and the Network for the Detection of Atmospheric Composition Change (NDACC) and are publicly available: http://woudc.org/data/explore.php , ftp://ftp.cpc.ncep.noaa.gov/ndacc/station/lauder/ames/o3sonde/ . |
| <u>Surface-based remote sensing</u> | |
| Table Mountain lidar | Data used in this publication are archived with NDACC and are publicly available (see http://www.ndacc.org ; Leblanc, 2016). For additional data or information please contact the authors. Leblanc, T.: TMO lidar data at NDACC database, available at: ftp://ftp.cpc.ncep.noaa.gov/ndacc/station/tmo/ames/lidar/ , last access: 25 July 2016. |
| OHP ozonesondes and lidar | Data used in this publication are archived with NDACC and are publicly available: http://www.ndacc.org |
| FTIR | Profiles with 40-50 levels archived at NDACC database: http://www.ndsc.ncep.noaa.gov/data/ , https://www2.acom.ucar.edu/irwg |
| Umkehr | http://www.woudc.org/ |
| <u>Satellite products</u> | |
| OMI/MLS | Monthly gridded data at 1°x1.25° resolution available from NASA Goddard Space Flight Center: https://acd-ext.gsfc.nasa.gov/Data_services/cloud_slice/ |
| GOME and OMI from SAO | Monthly GOME gridded data are available at https://www.cfa.harvard.edu/~xliu/res/gmtrop.htm . Monthly gridded data at 1°x1.25° resolution are derived from OMI OMPROFOZ data. OMI OMPROFOZ data are available from Aura Validation Data Center, NASA Goddard Space Flight Center: https://avdc.gsfc.nasa.gov/index.php?site=1389025893&id=74 |
| OMI-RAL | Archive under development |
| IASI-FORLI | http://cds-espri.ipsl.upmc.fr/etherTypo/index.php?id=1719&L=1 |
| IASI-SOFRID | v1.5 ozone data are available online at http://thredds.sedoo.fr/iasi-sofrid-o3-co/ |

| | |
|---|--|
| SCIAMACHY | Data are available from the Institute of Environmental Physics, University of Bremen on request |
| IASI LWRE | Archive under development |
| IASI-LISA | Data are available from the Laboratoire Interuniversitaire des Systèmes Atmosphériques (LISA, CNRS-UPEC-UPD) upon request. Contact: cuesta@lisa.u-pec.fr |
| IASI+GOME2, LISA | These data are now being produced routinely and will soon be available at http://www.aeris-data.fr . Until then, the data will be made available from the Laboratoire Interuniversitaire des Systèmes Atmosphériques (LISA, CNRS-UPEC-UPD) upon request. Contact: cuesta@lisa.u-pec.fr |
| TES | Ozone vertical profiles, total column, tropospheric column for single observations with 5km x 8km horizontal resolution (L2) and daily/monthly averaged, gridded (L3) products. Global observations for 2004-2009; Megacity and other regions of interest for 2010-present. available at: https://eosweb.larc.nasa.gov/project/tes/tes_table |
| TOR (Tropospheric Ozone Residual satellite product) | Monthly gridded data at 1°x1.25° resolution available from NASA Langley Research Center: https://science.larc.nasa.gov/TOR/ |

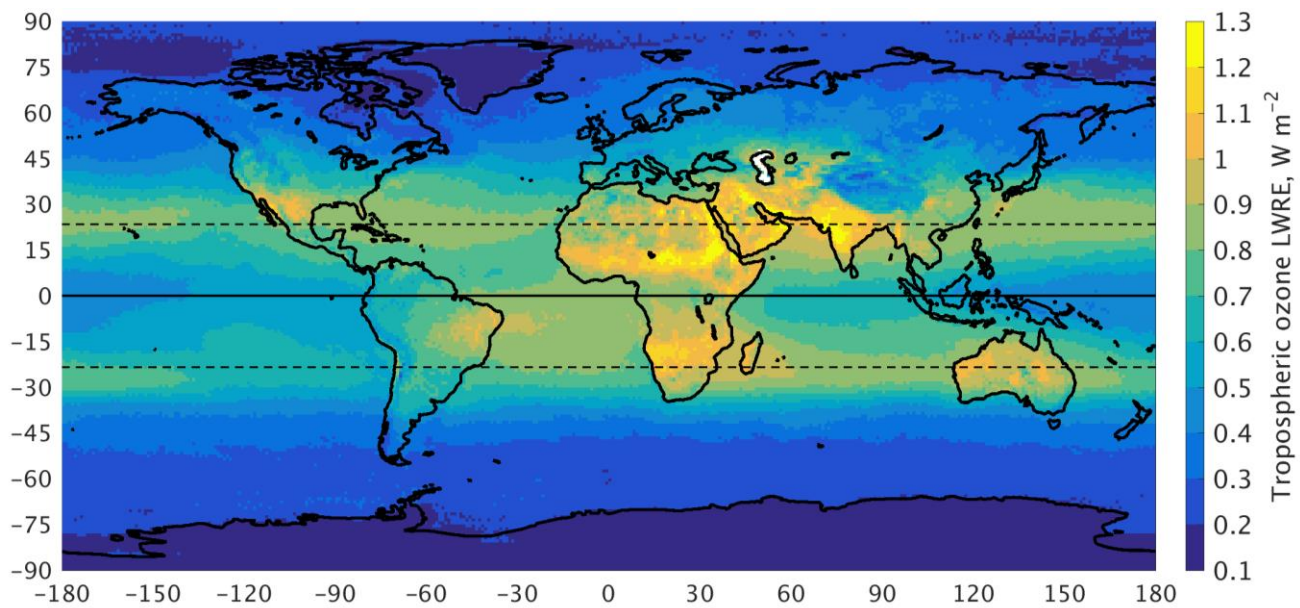


Figure 1.2 Clear-sky (cloud cover < 13%) ozone LWRE (W m^{-2}) as estimated from IASI measurements shows the present day greenhouse effect of tropospheric ozone. The spatial variability of LWRE is due to variations in tropospheric ozone, surface temperature, atmospheric temperature and water vapor. Data are averaged from December 2014 to November 2015 on a $1^\circ \times 1^\circ$ grid.

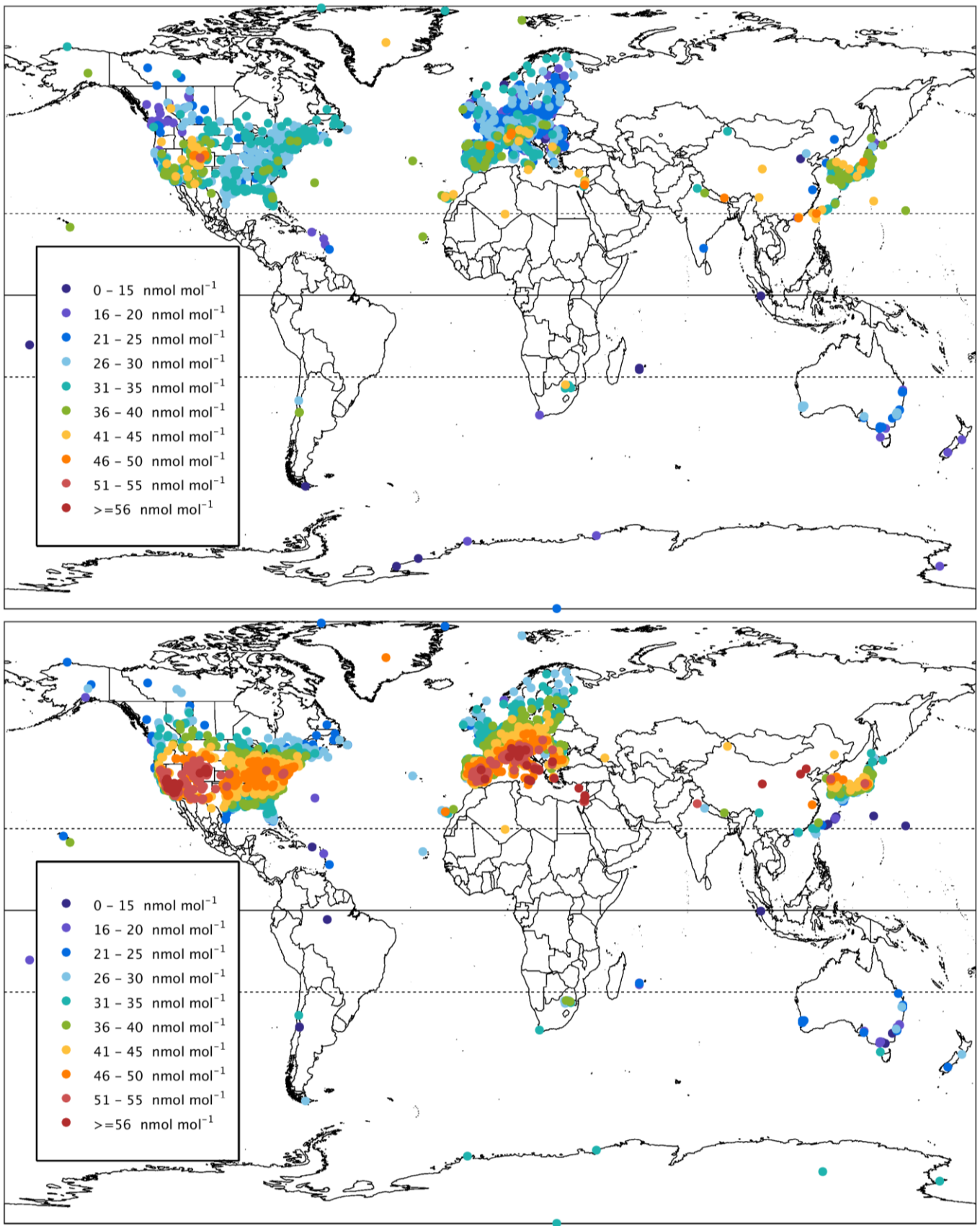
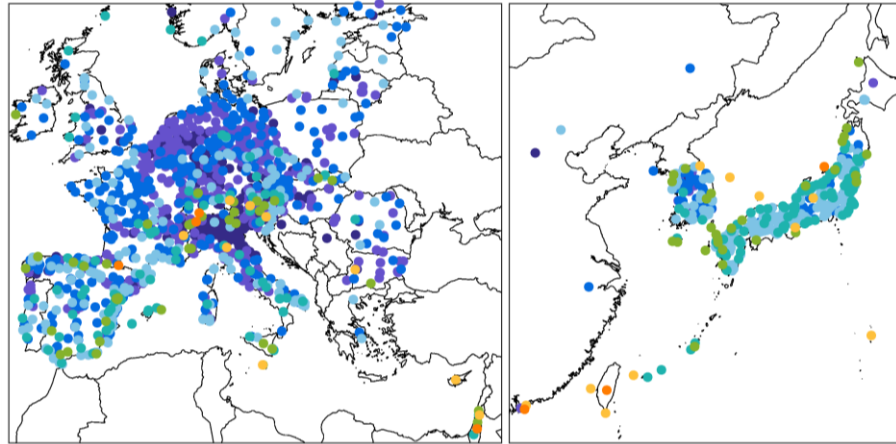
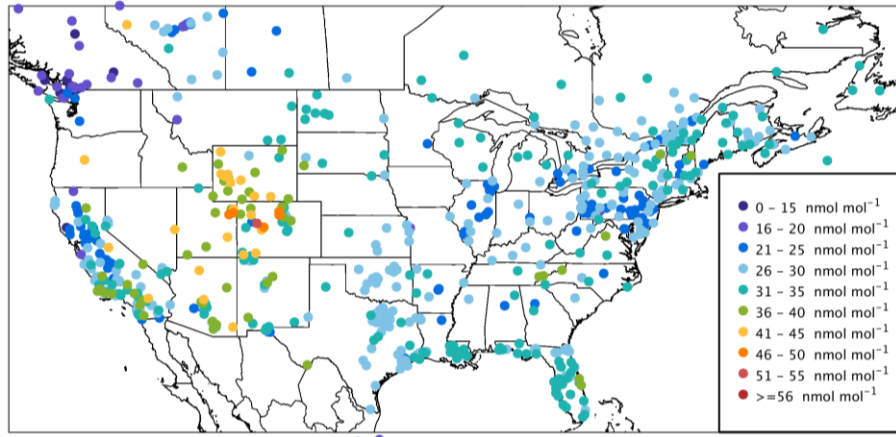
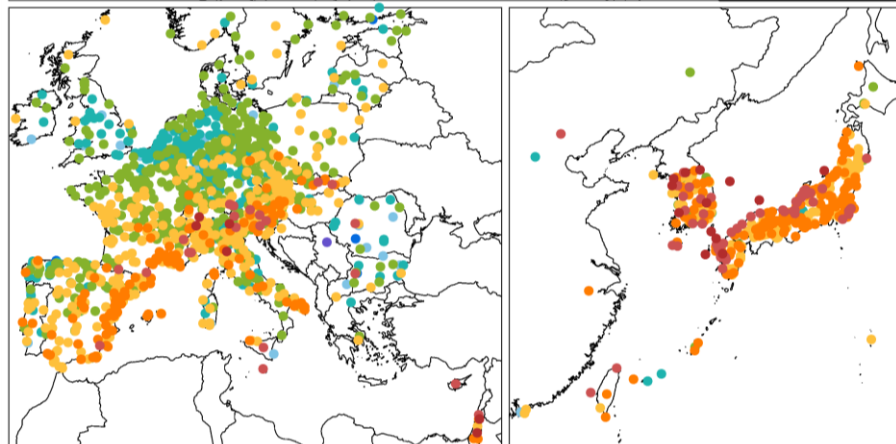
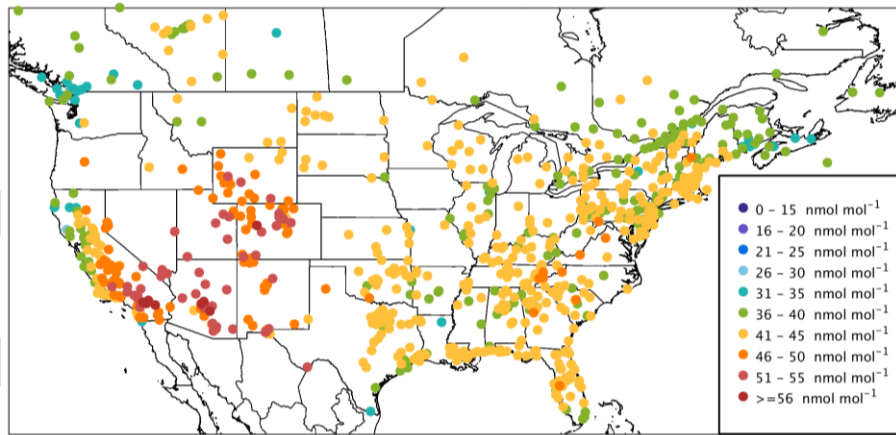


Figure 3.1.1 Daytime average ozone (nmol mol^{-1}) at 2702 non-urban surface sites in December-January-February (top) and 3136 non-urban sites in June-July-August (bottom) for the present-day period, 2010-2014.



a



b

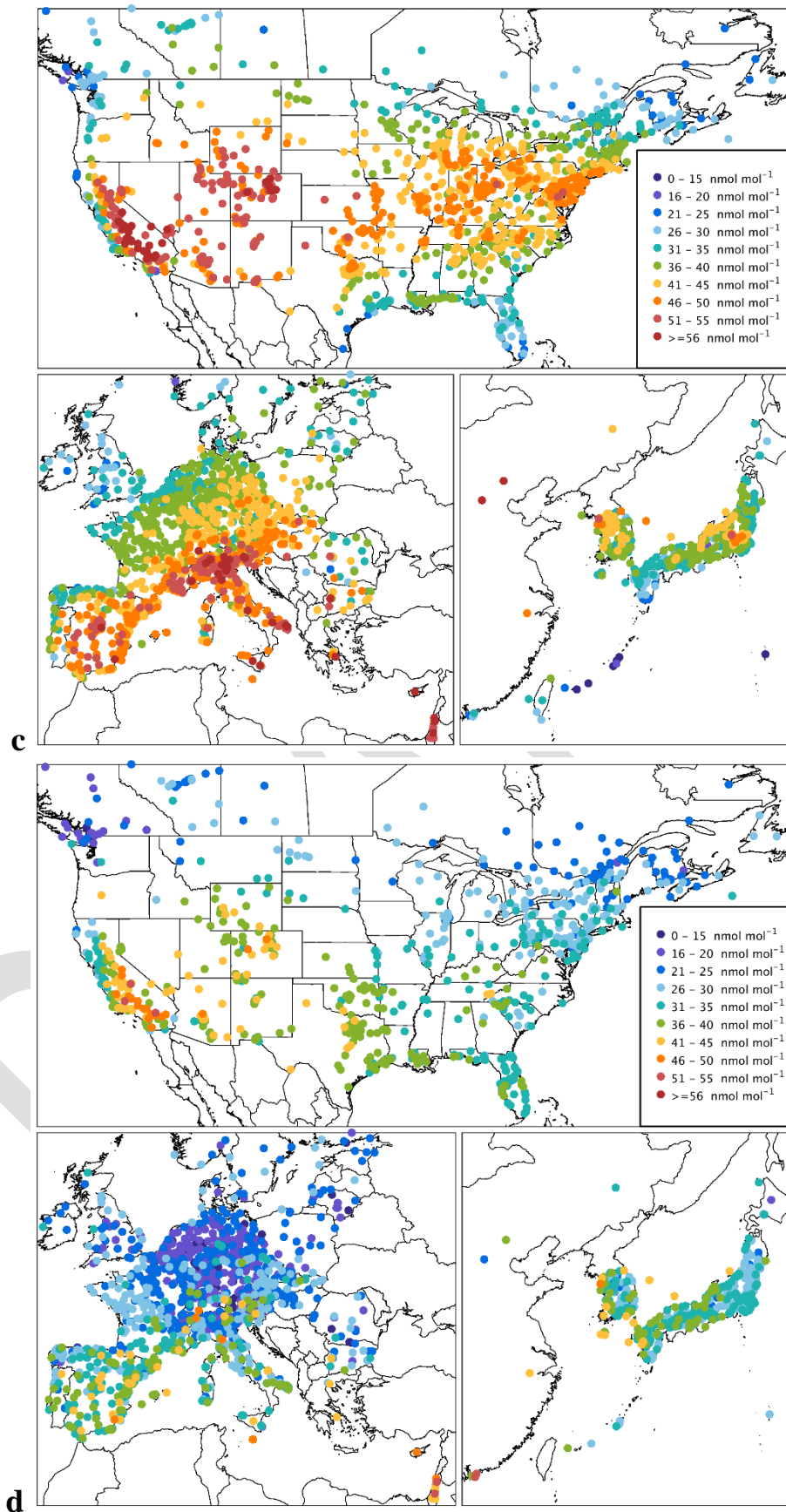


Figure 3.1.2 Daytime average ozone (nmol mol⁻¹) at all available non-urban surface sites for DJF (a), MAM (b), JJA (c) and SON (d), for the present-day period, 2010-2014. Panels (a) and (c) show the same data as Figure 3.1.1 (top and bottom, respectively), but focus on the three regions with dense surface networks.

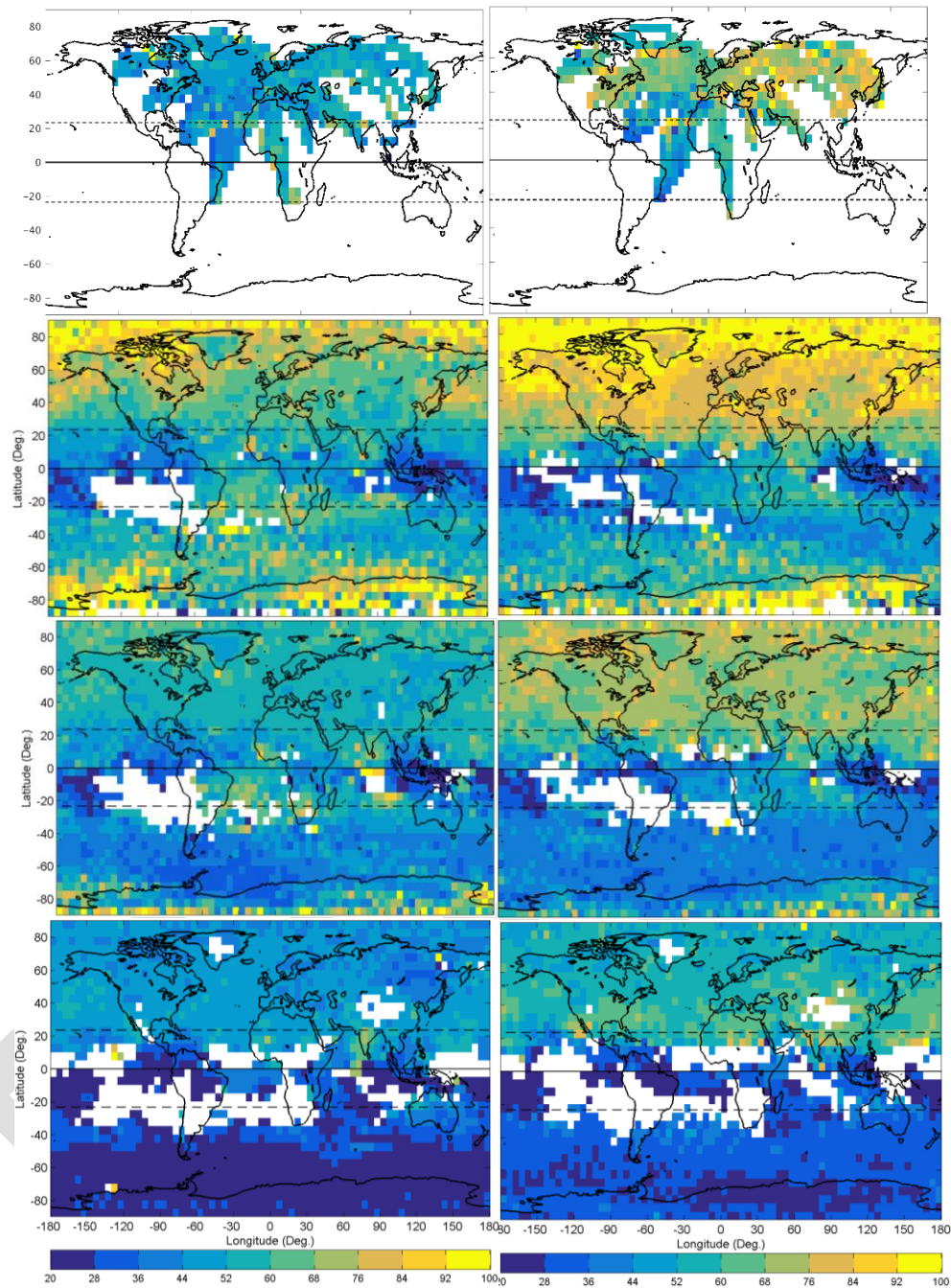


Figure 3.2.1 Mean ozone (nmol mol^{-1}) at four levels in the free troposphere as measured by IAGOS commercial aircraft (2009-2013) at 9-12 km (UT), but below the dynamical tropopause (top row), and as measured by ozonesondes (data from 2008-2012 spatially distributed using the TOST method) at 7-9 km (2nd row), 5-7 km (3rd row) and 2-3 km (bottom row). White areas indicate no data. Data are displayed seasonally for DJF (left) and MAM (right)...*figure continued on next page.*

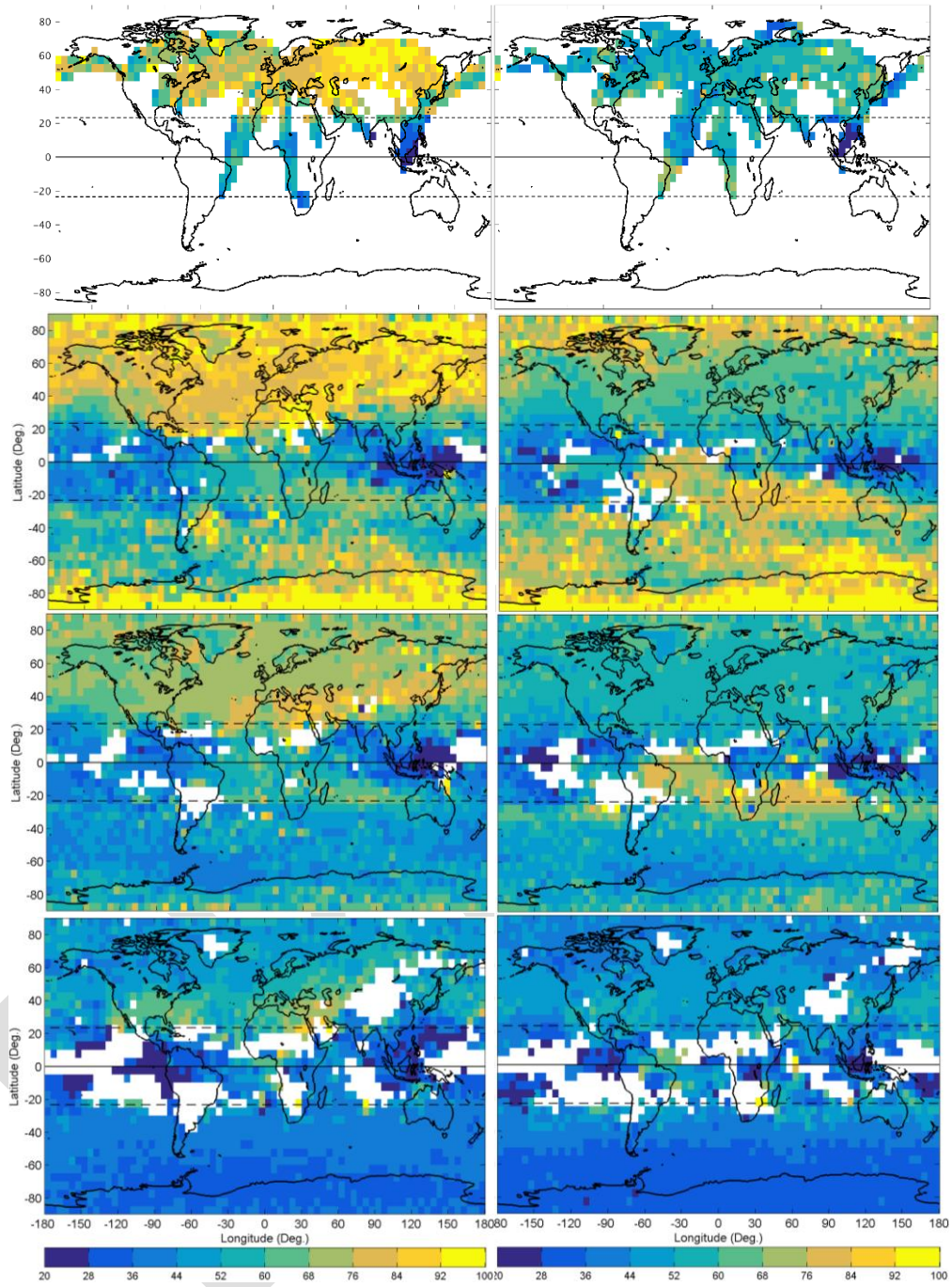


Figure 3.2.1 ... continued: JJA (left) and SON (right).

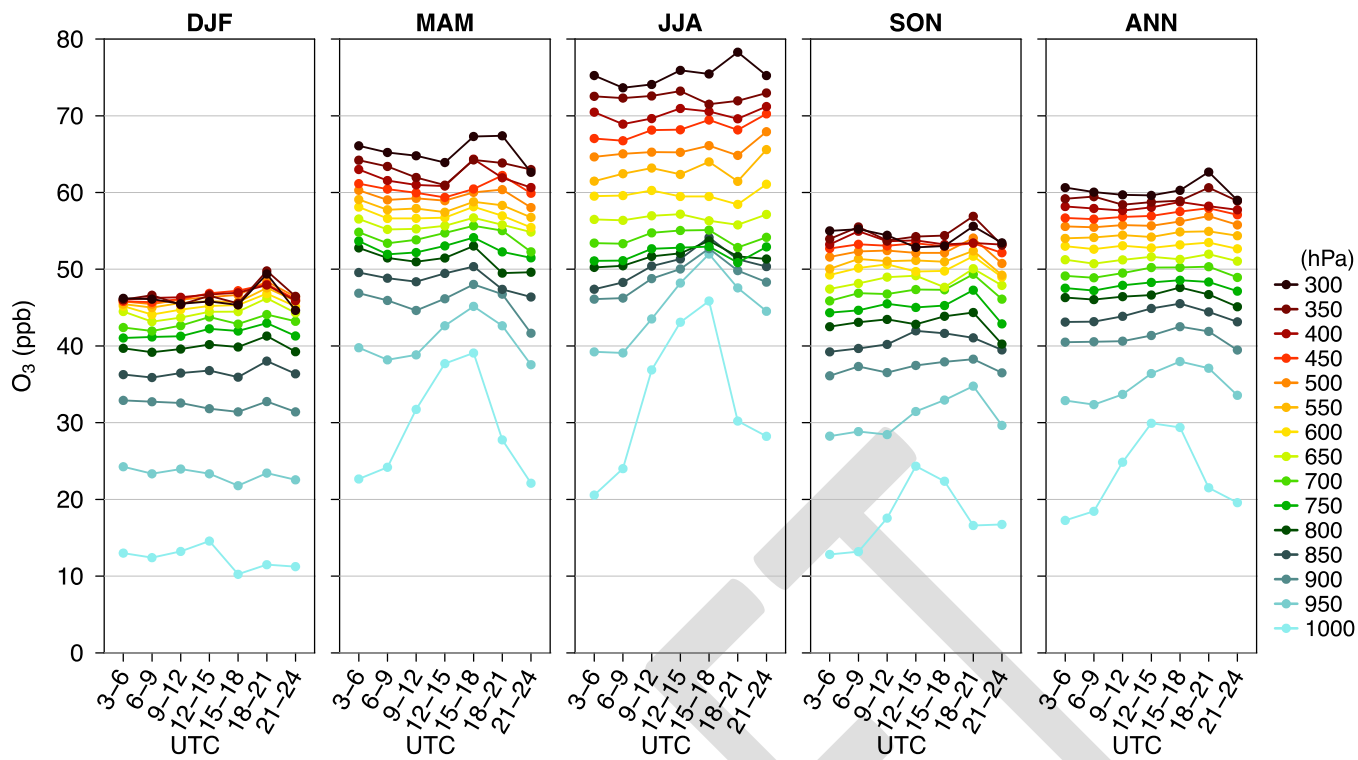


Figure 3.2.2 Diurnal variability of mean tropospheric ozone from the surface to the tropopause above Frankfurt between August 1994 and December 2012, by season and annually (ANN: annual). Reproduced with authorization from the authors of *Petetin et al.* (2016).

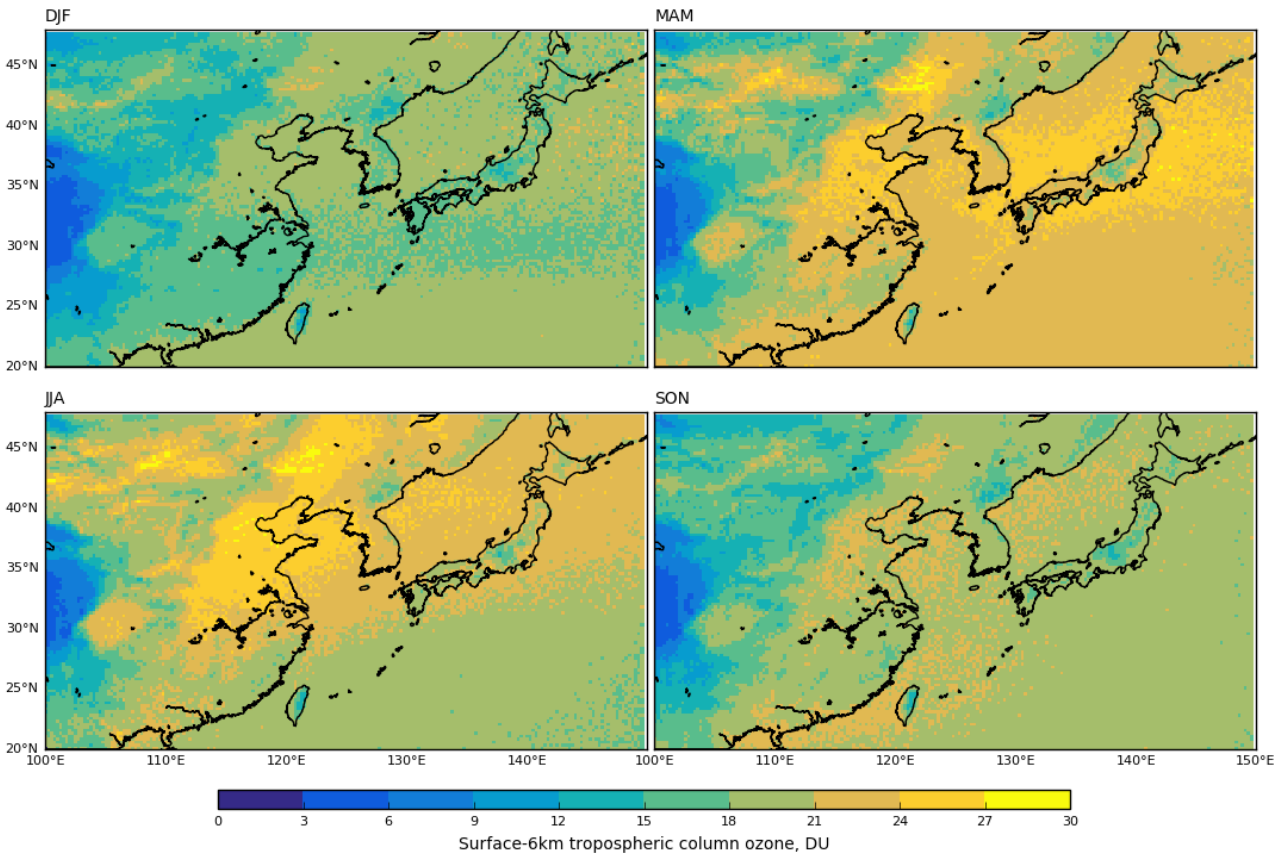
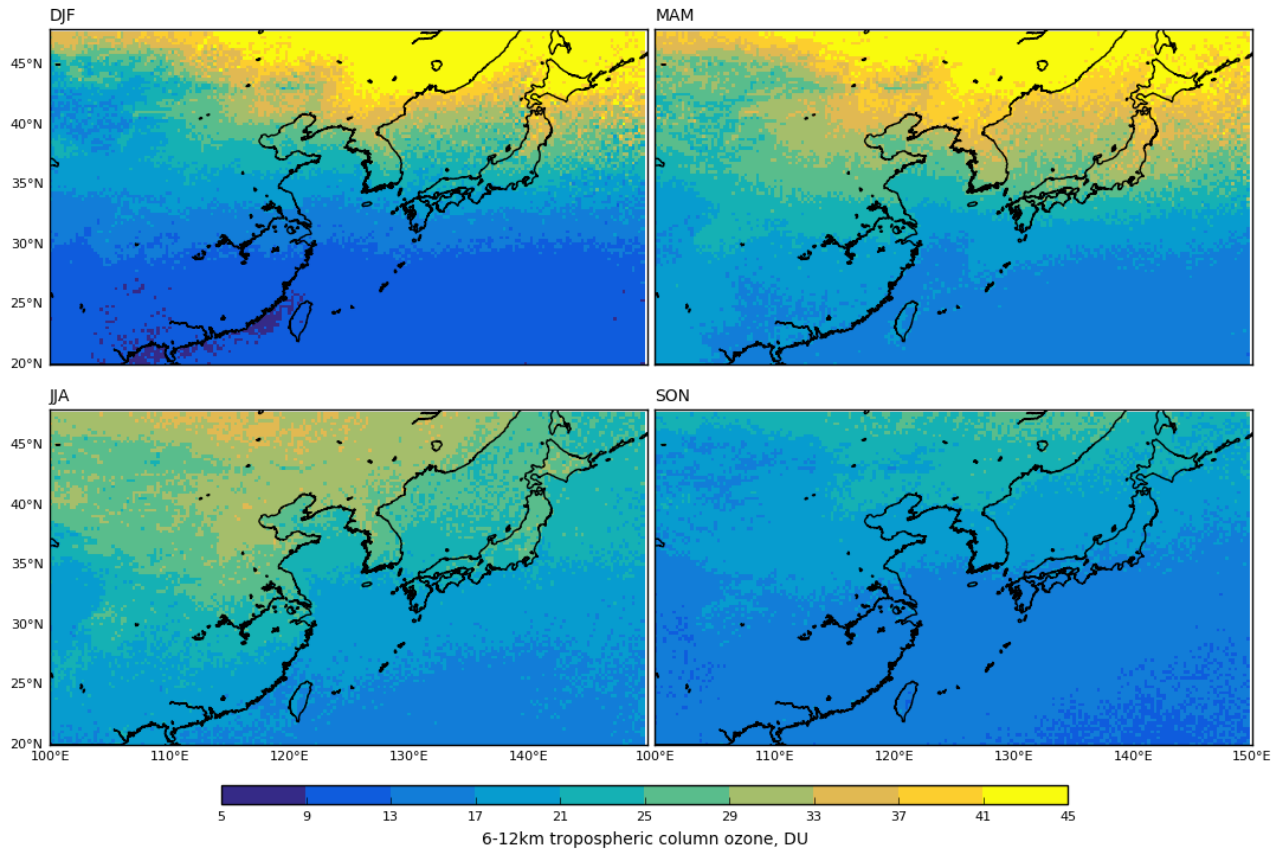


Figure 3.3.1 Seasonal 6-12 km (top) and surface-6 km (bottom) partial ozone columns (DU) over East Asia, according to the IASI-LISA (TP) product for 2010-2014.

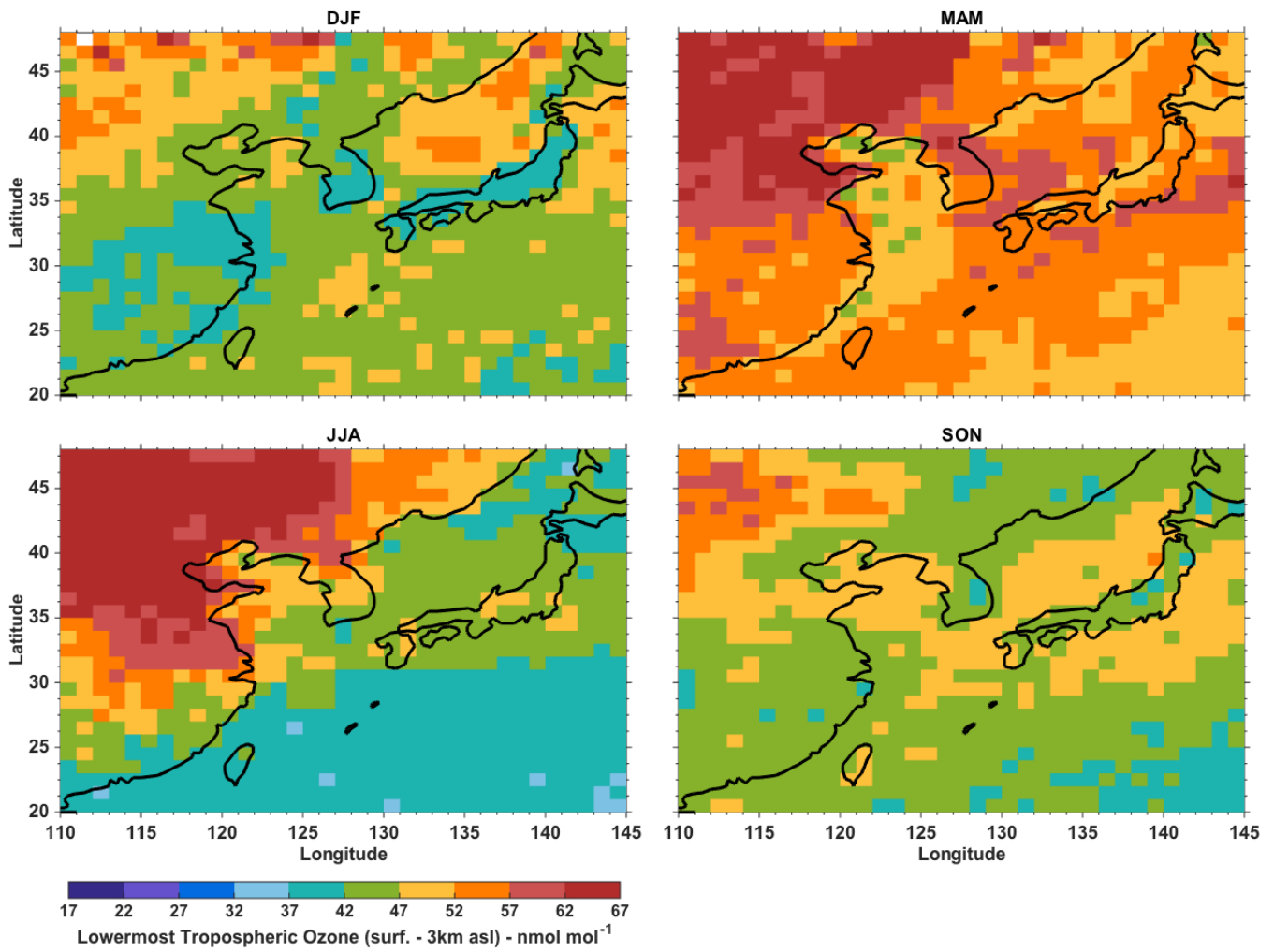


Figure 3.3.2 IASI+GOME2 (LISA) seasonal (2010) average ozone mole fraction (nmol mol^{-1}) over East Asia from the surface to 3 km. Horizontal resolution is $1^\circ \times 1^\circ$.

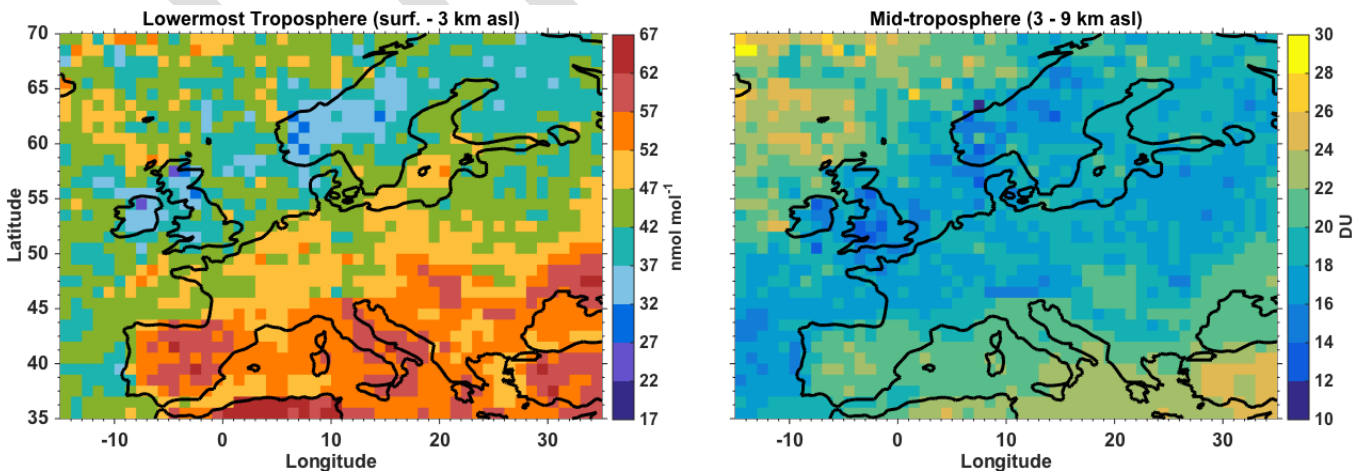


Figure 3.3.3 IASI+GOME2 (LISA) monthly average (August, 2009) mixing ratio (nmol mol^{-1}) from the surface to 3 km (left) and partial column ozone (DU) from 3 to 9 km (right) over Europe. Horizontal resolution is $0.5^\circ \times 0.5^\circ$ and the data are smoothed using a horizontal moving average of 1.5° .

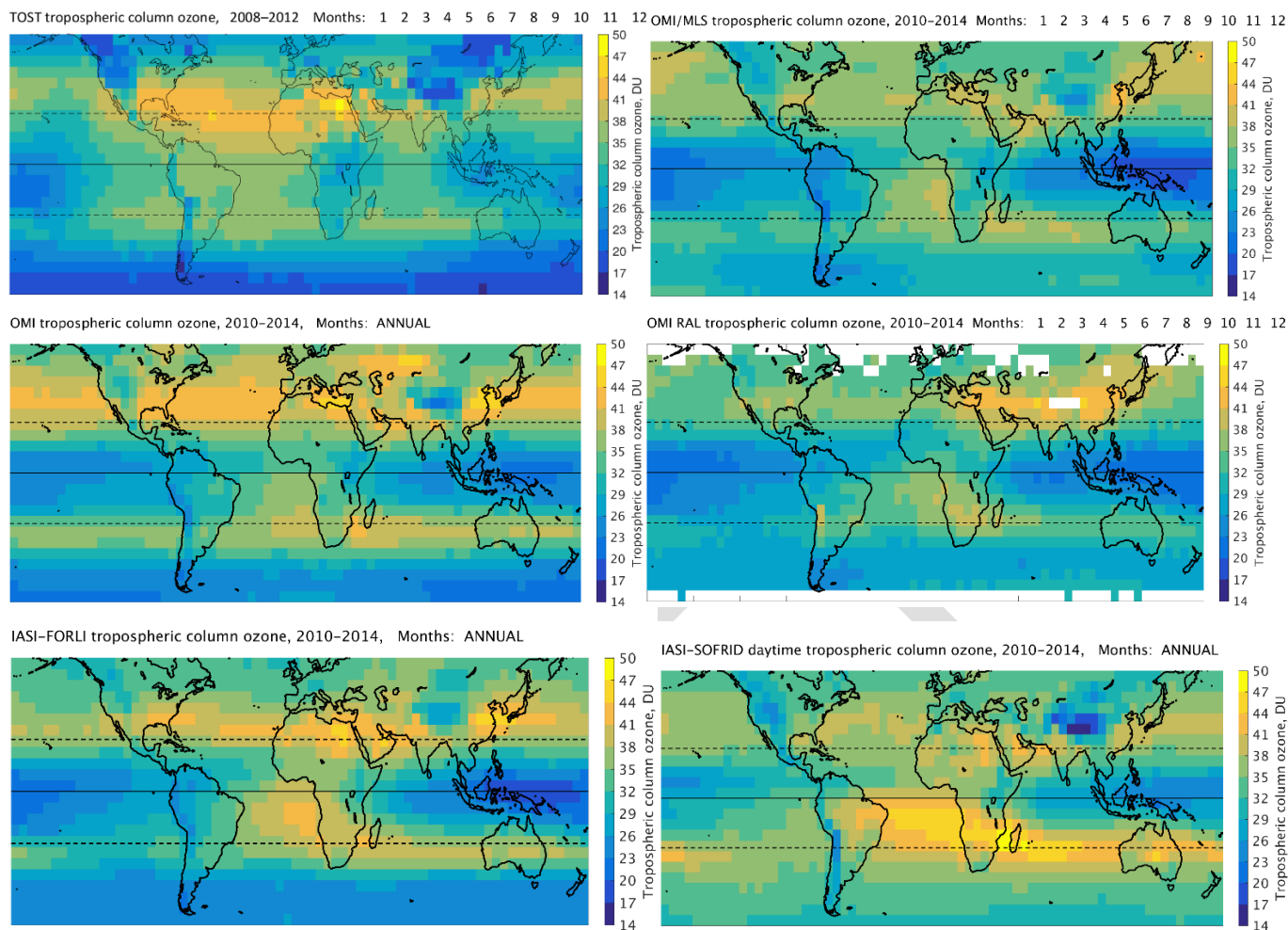


Figure 3.4.1 Annual mean tropospheric column ozone (DU) as measured by TOST (top left), OMI/MLS (top right, with + 2 DU offset to account for bias), OMI-SAO (middle left), OMI-RAL (middle right), IASI-FORLI (bottom left) and IASI-SOFRID (bottom right). The data are averaged over the period January 2010 through December 2014 and reported at $5^{\circ} \times 5^{\circ}$ horizontal resolution, except for TOST, which covers the period 2008-2012.

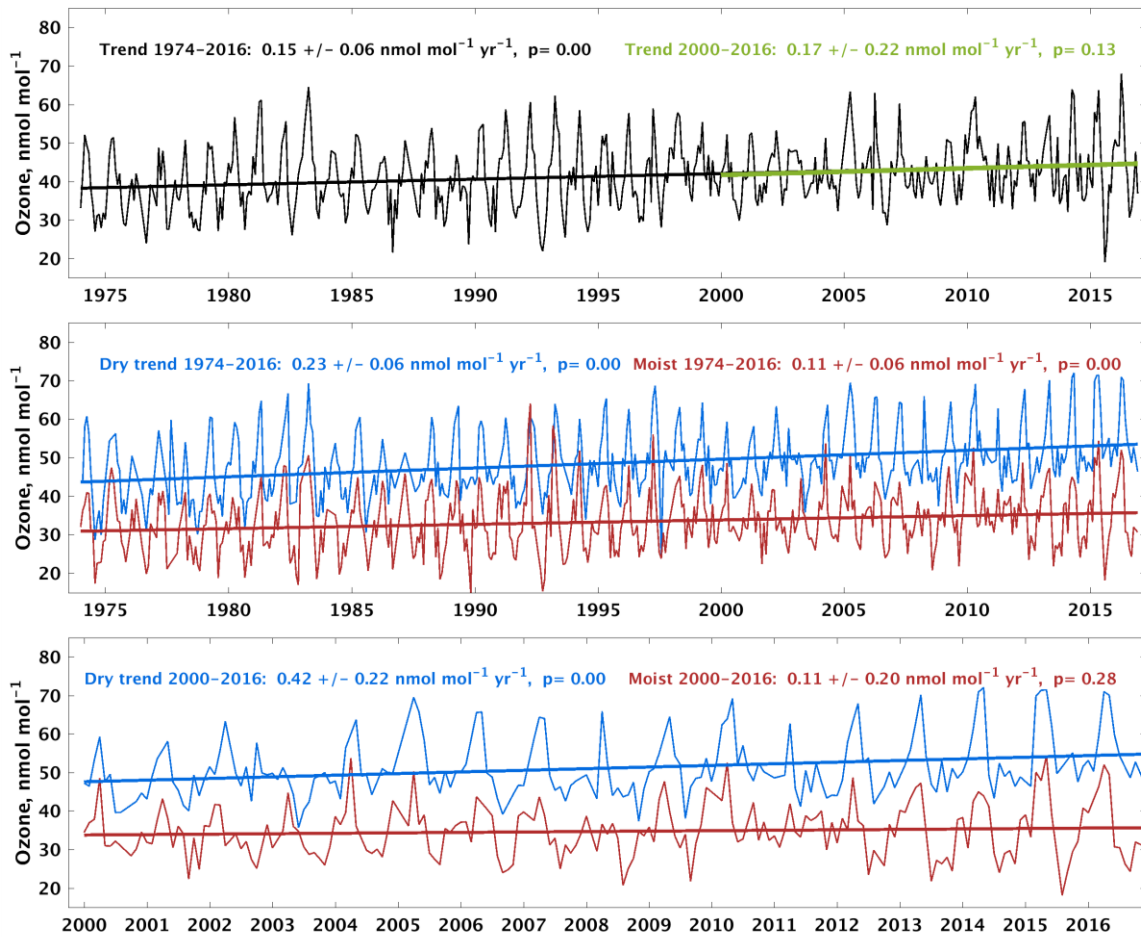


Figure 4.1.1 a) Nighttime monthly median ozone values at Mauna Loa Observatory calculated with all available data for months with at least 50% data availability, January 1974 – December 2016. b) Same as in a) but for data split into dry (dewpoint less than the climatological monthly 40th percentile) and moist (dewpoint greater than the climatological monthly 60th percentile) categories. A dry or moist category in any given month must have a sample size of at least 24 individual hourly nighttime observations. c) As in b) but for 2000–2016. Trends in this figure are based on least-squares linear regression fit through the monthly median values, and reported with 95% confidence intervals and p-values.

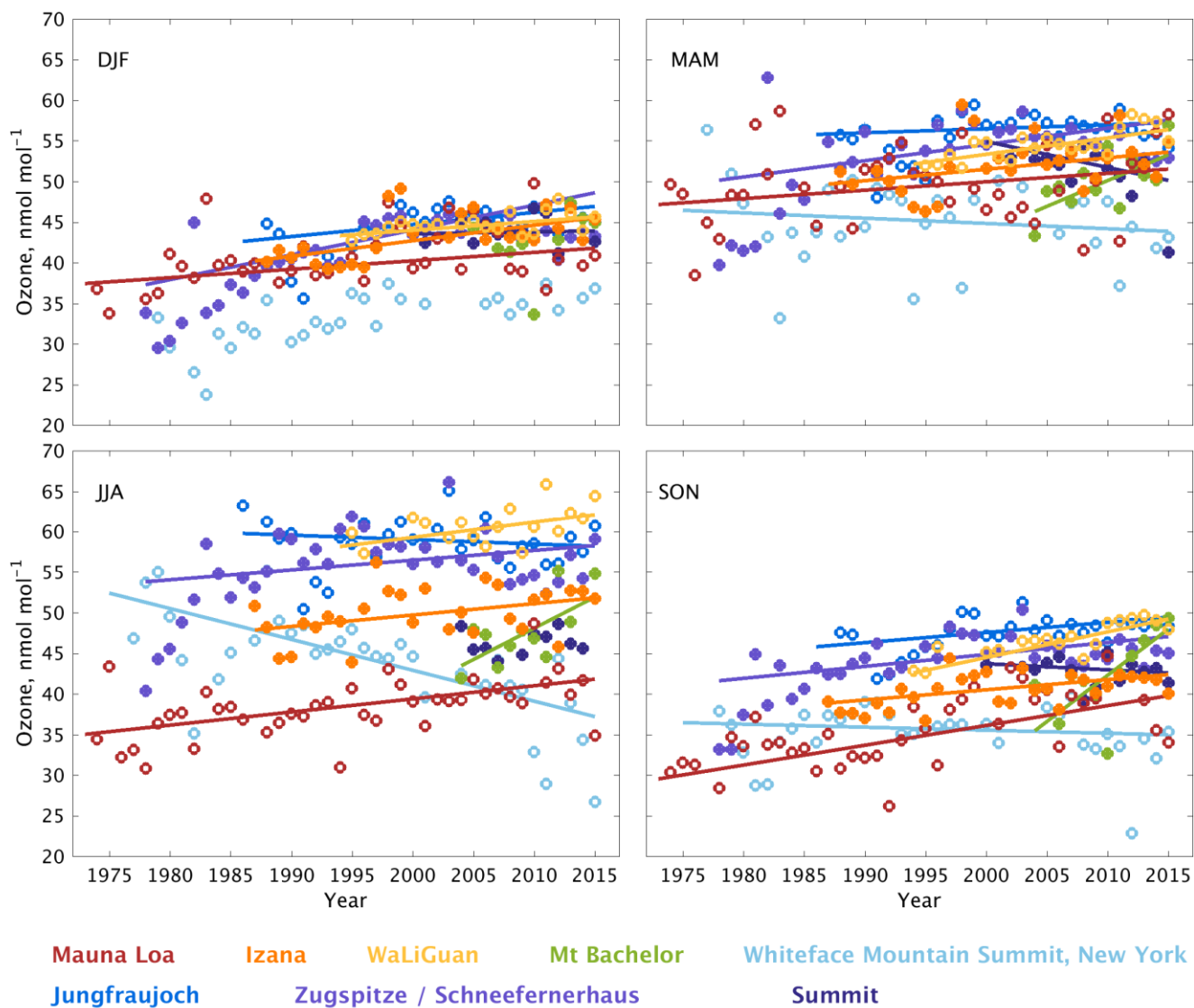


Figure 4.1.2 Nighttime ozone trends at eight Northern Hemisphere mountaintop sites by season. Trend values are given in Table 4.1.

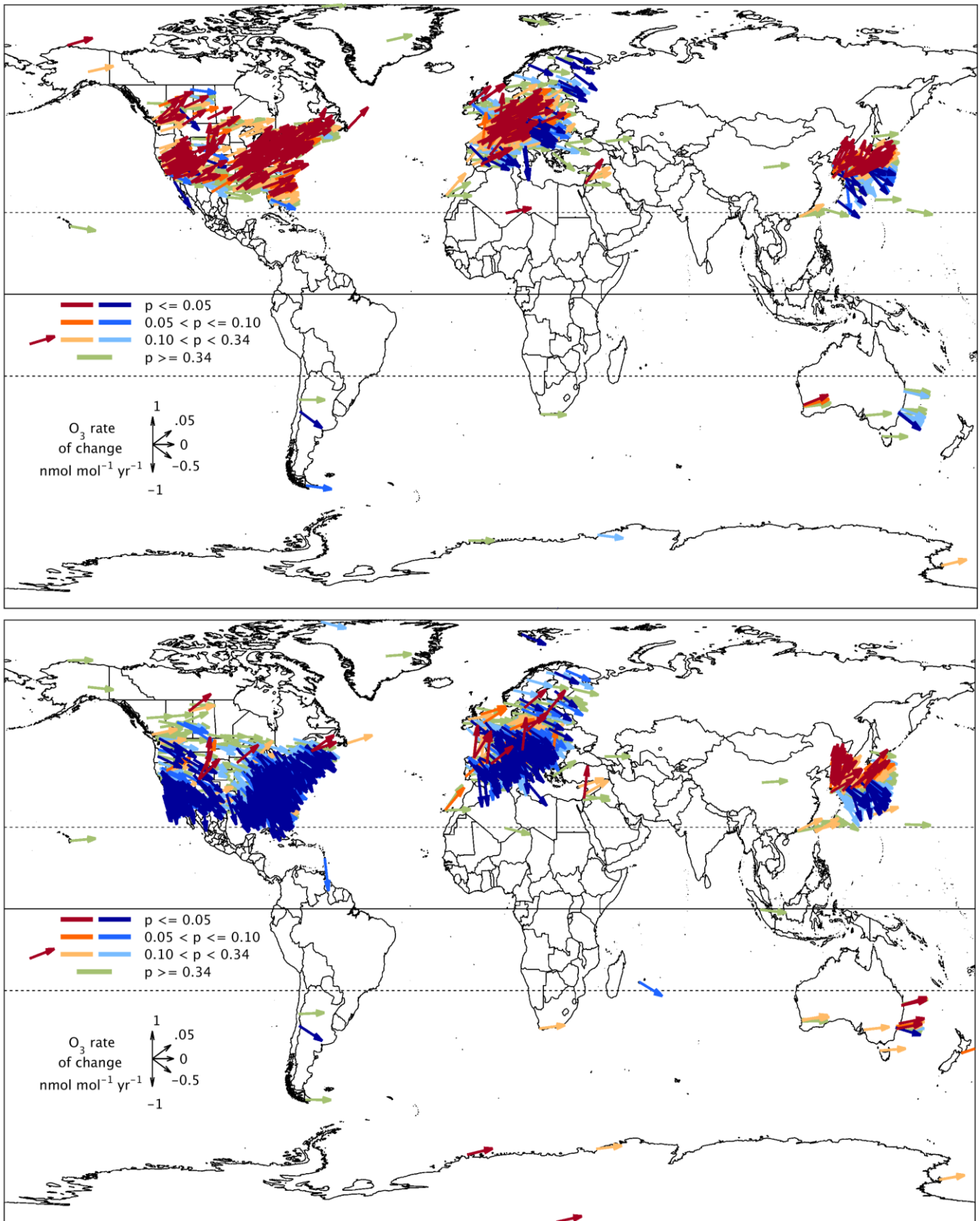
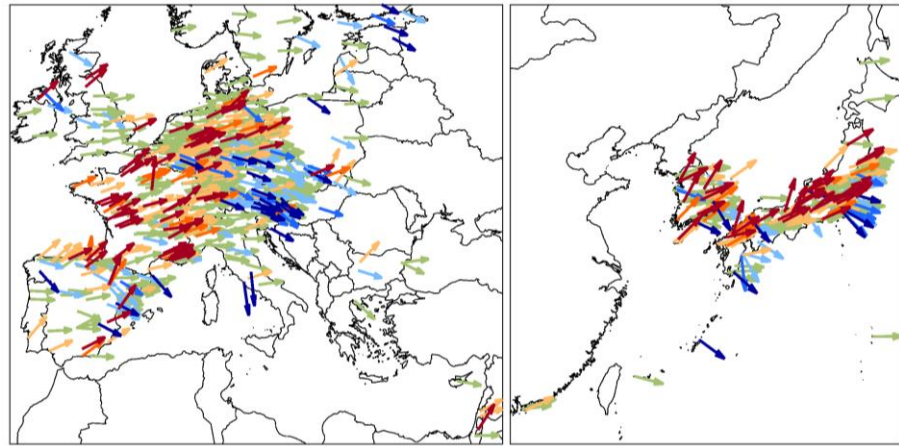
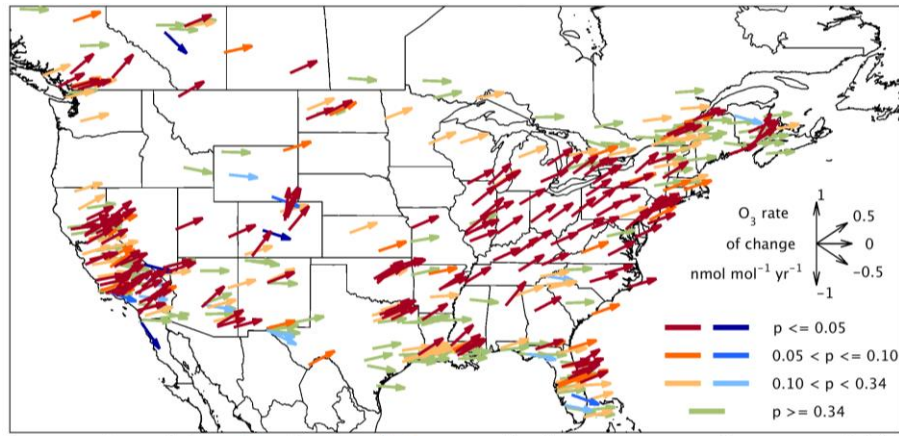
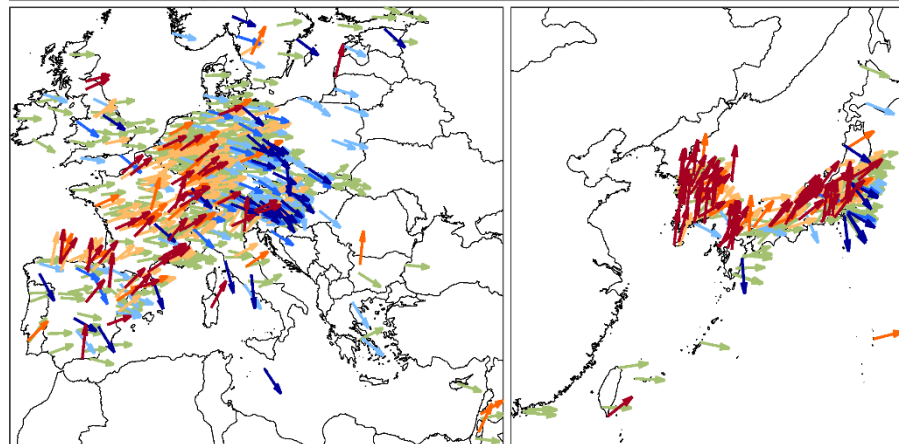
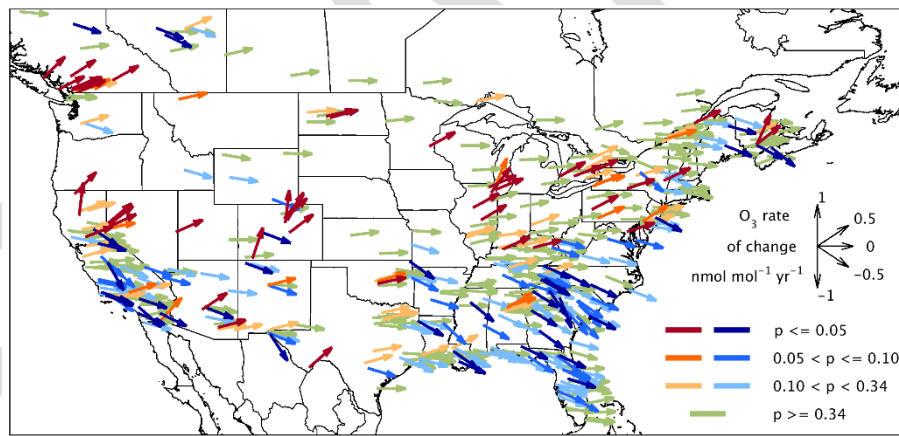


Figure 4.1.3 2000-2014 trends of daytime average ozone (nmol mol^{-1}) at 1375 non-urban sites in December-January-February (top) and 1784 non-urban sites in June-July-August (bottom). The number of available sites is greater in June-July-August because many US sites only operate in the warm season. Vector colors indicate the p-values on the linear trend for each site: blues indicate negative trends, oranges indicate positive trends and green indicates weak or no trend; lower p-values have greater color saturation.



a.



b.

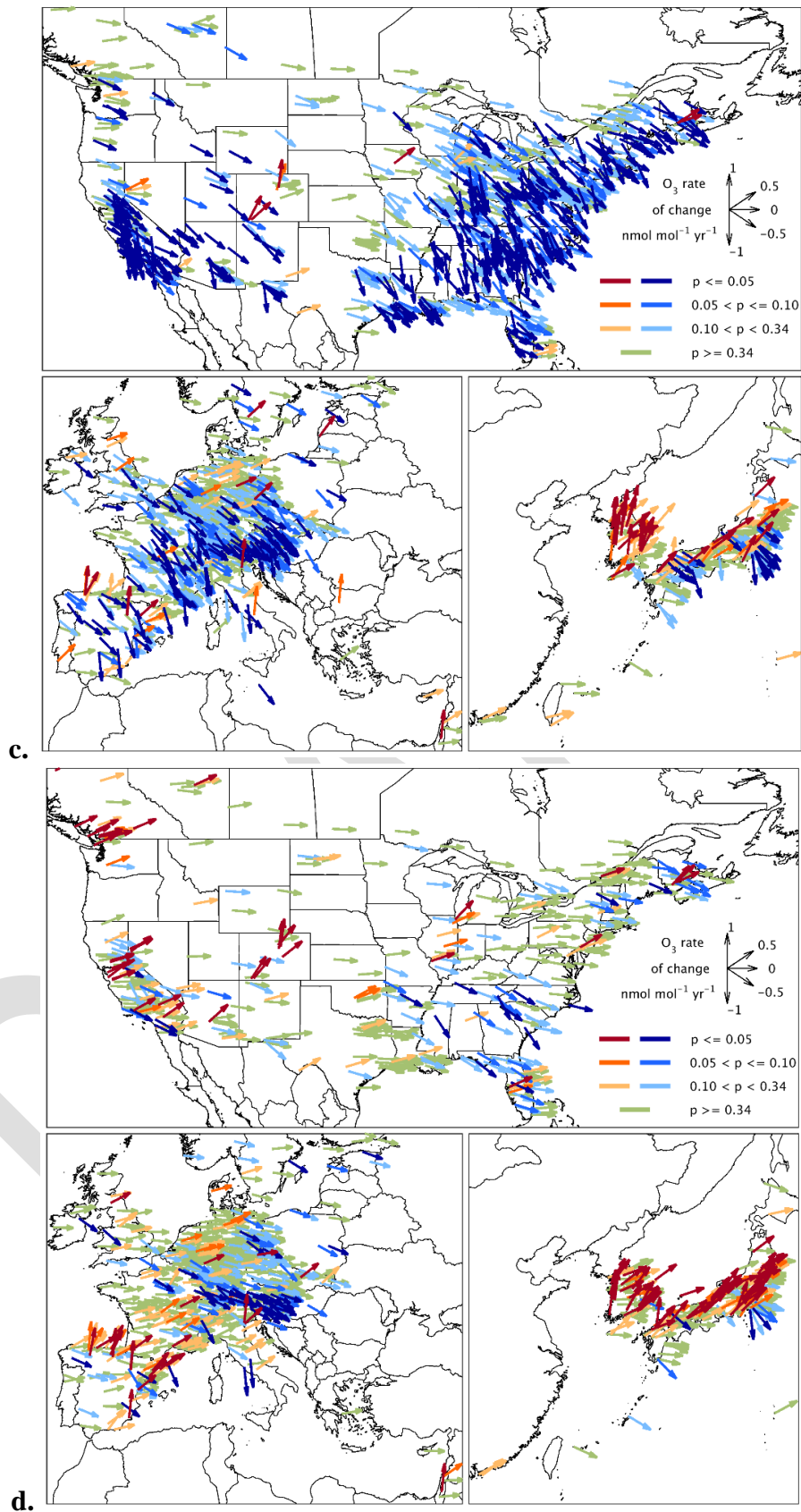


Figure 4.1.4 Regional trends (2000-2014) of daytime average ozone (nmol mol⁻¹ yr⁻¹) at all non-urban sites for Dec-Jan-Feb (a), Mar-Apr-May (b), Jun-Jul-Aug (c) and September-October-November (d). Vector colors indicate the p-Values on the linear trend for each site: blues indicate negative trends, oranges indicate positive trends and green indicates weak or no trend.

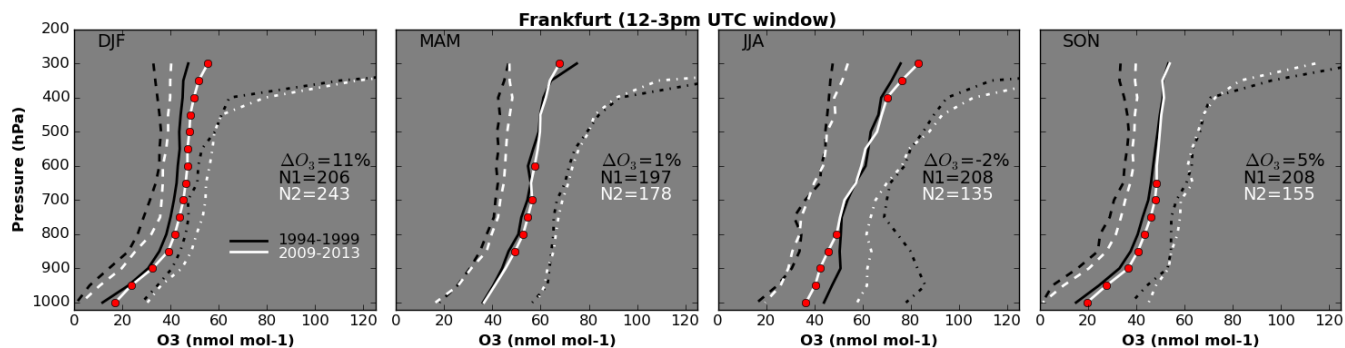


Figure 4.2.1 Seasonal changes of ozone above Frankfurt, Germany, based on MOZAIC/IAGOS aircraft profiles over the periods 1994-1999 (black lines) and 2009-2013 (white lines) for the 5th, 50th and 95th percentiles. Red dots indicate a statistically significant difference at that level between the two periods, based on a t-test and a 95% confidence interval. Percent changes of ozone are reported for the mass of ozone from the surface to 300 hPa.

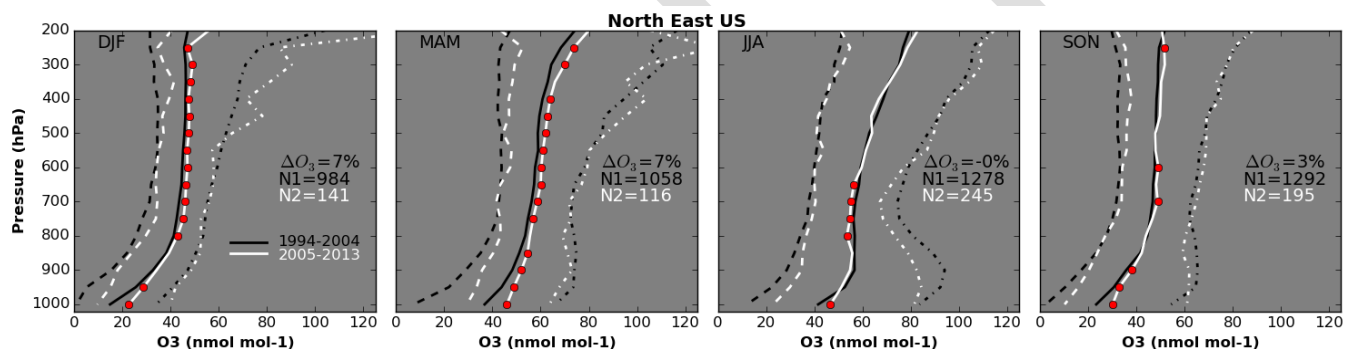


Figure 4.2.2 Seasonal change in the 5th, 50th and 95th ozone percentiles above the northeastern USA, based on MOZAIC/IAGOS aircraft profiles from 1994-2004 (black lines) to 2005-2013 (white lines) as measured by lidar. Red dots indicate a statistically significant difference at that level between the two periods, based on a t-test and a 95% confidence interval. ΔO_3 values refer to the change in tropospheric ozone mass between the two periods.

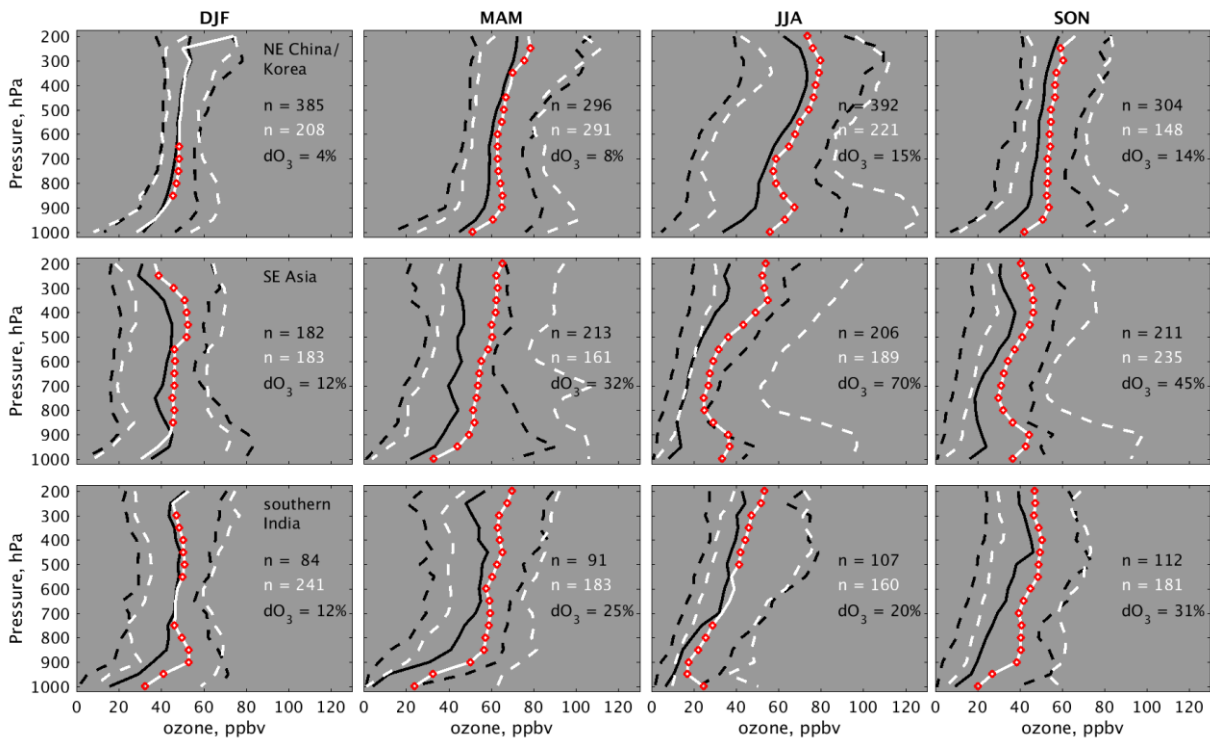


Figure 4.2.3 Ozone profiles above northeastern China (30°-43°N, 110°-129°E), Southeast Asia (10°-24°N, 93°-115°E), and south/central India (6°-24°N, 70°-89°E) based on observations from IAGOS commercial aircraft to and from several airports in each region. In addition, SE Asia includes ozonesonde profiles from the SHADOZ station in Hanoi, Vietnam. Shown are the 50th (solid lines) and 5th and 95th percentiles (dashed lines) for the periods 1994-2004 (black) and 2005-2014 (white). Layers in which there is a statistically significant ozone difference between the two time periods are indicated by red circles, based on a t-test and a 95% confidence interval. Each panel indicates the percent increase in the tropospheric ozone mass (1000-200 hPa) from the earlier to the later period, as well as the number (n) of vertical profiles associated with each region and time period. These results were first reported by Zhang *et al.* (2016).

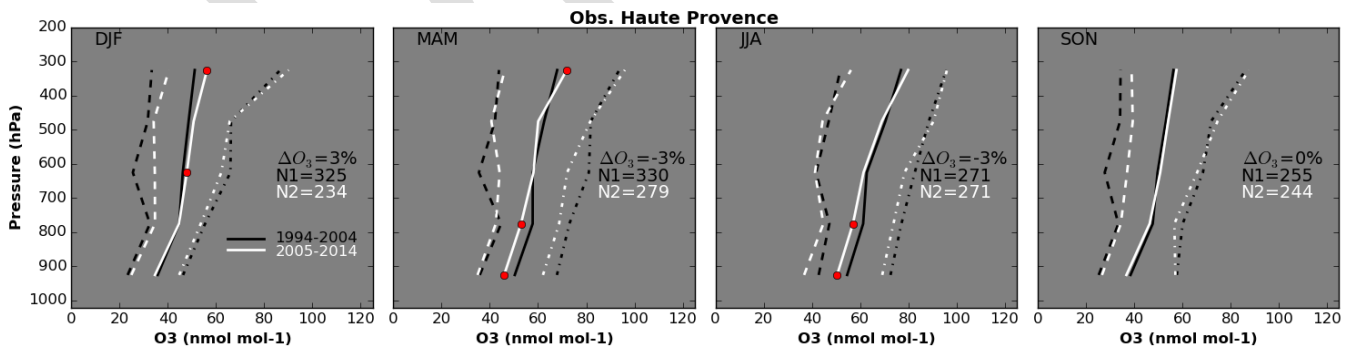


Figure 4.2.4 Seasonal change in the 5th, 50th and 95th ozone percentiles above Observatoire de Haute Provence, France, from 1994-2004 (black lines) to 2005-2014 (white lines) as measured by a combination of lidar and ozonesonde profiles. Red dots indicate a statistically significant difference at that level between the two periods, based on a t-test and a 95% confidence interval. ΔO_3 values refer to the change in tropospheric ozone mass between the two periods. An update to Gaudel *et al.* (2015).

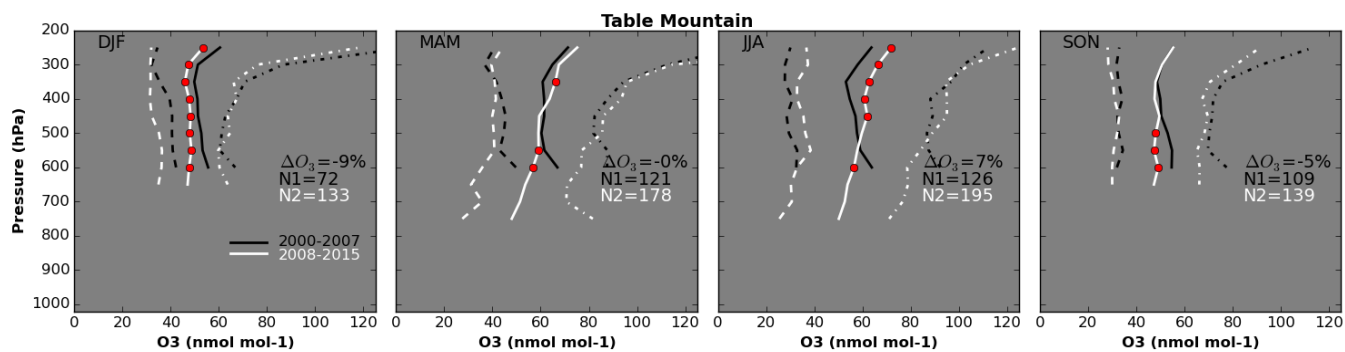


Figure 4.2.5 Seasonal change in the 5th, 50th and 95th ozone percentiles above Table Mountain, southern California, from 2000-2007 (black lines) to 2008-2015 (white lines) as measured by lidar. Red dots indicate a statistically significant difference at that level between the two periods, based on a t-test and a 95% confidence interval. ΔO_3 values refer to the change in tropospheric ozone mass between the two periods. An update to *Granados-Muñoz et al.* (2016).

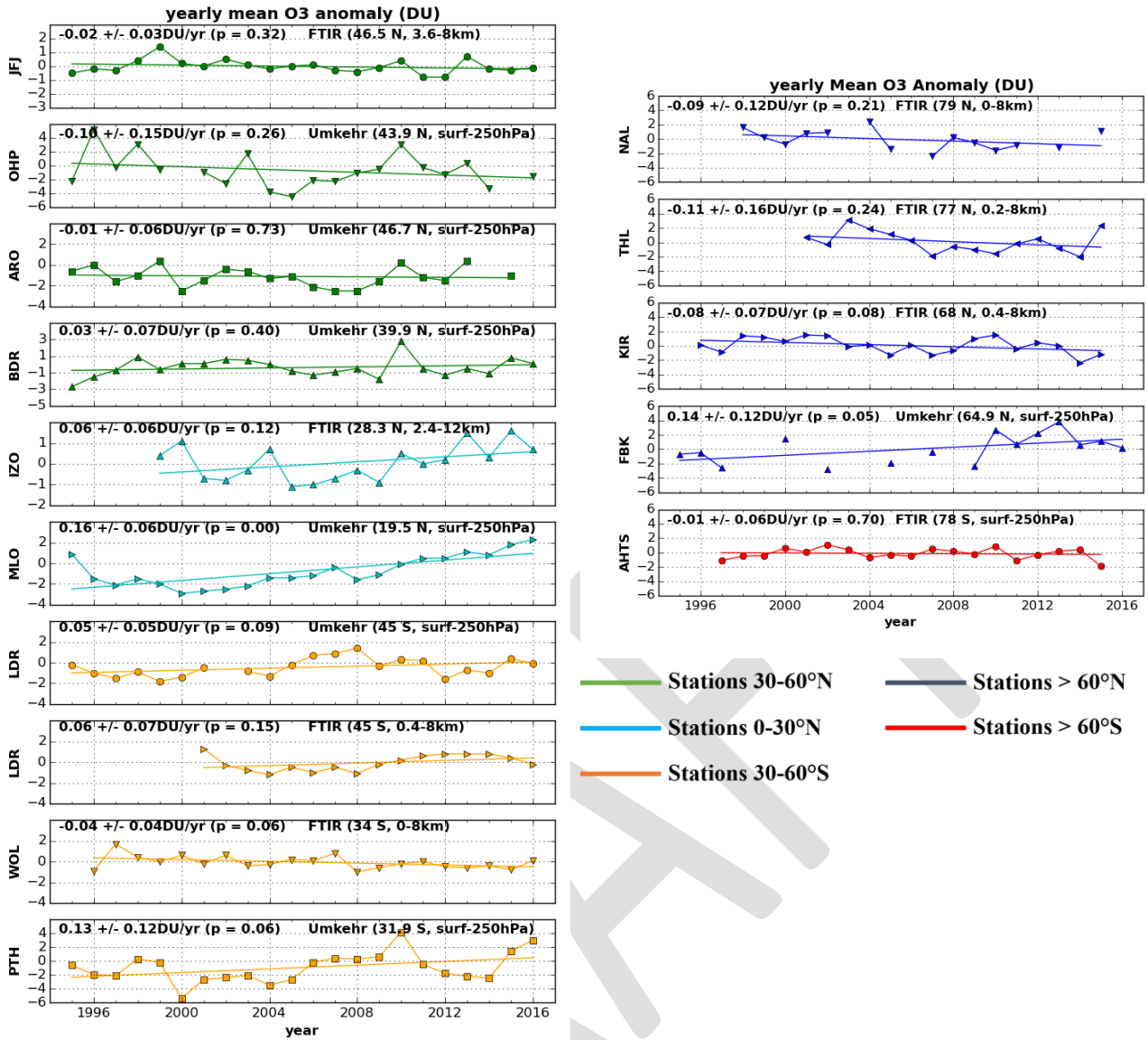


Figure 4.2.6 Trends of TCO anomalies (DU) measured by FTIR and Umkehr above thirteen stations: Jungfrauoch (JFJ), Observatoire de Haute Provence (OHP), Boulder (BDR), Izaña (IZO), Mauna Loa (MLO), Lauder (LDR), Wollongong (WOL), Perth (PTH), Ny-Ålesund (NAL), Thule (THL), Kiruna (KIR), Fairbanks (FBK) and Arrival Heights (AHTS). Colors indicate the latitude bands in which stations are located. Time series of TCO for latitude bands above 60°N or 60°S are shown in the right panel.